Profit benchmarking and degradation analysis for revenue stacking of batteries in Sweden's day-ahead electricity and frequency containment

Downloaded from: https://research.chalmers.se, 2025-03-22 17:45 UTC

Citation for the original published paper (version of record):
Mirzaei Alavijeh, N., Khezri, R., Mazidi, M. et al (2025). Profit benchmarking and degradation analysis for revenue stacking of batteries in Sweden's
day-ahead electricity and frequency containment reserve markets. Applied Energy, 381.
http://dx.doi.org/10.1016/j.apenergy.2024.125151

N.B. When citing this work, cite the original published paper.

research.chalmers.se offers the possibility of retrieving research publications produced at Chalmers University of Technology. It covers all kind of research output: articles, dissertations, conference papers, reports etc. since 2004. research.chalmers.se is administrated and maintained by Chalmers Library

(article starts on next page)

Applied Energy 381 (2025) 125151

Contents lists available at ScienceDirect

Applied Energy

journal homepage: www.elsevier.com/locate/apenergy

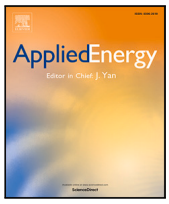

Profit benchmarking and degradation analysis for revenue stacking of batteries in Sweden's day-ahead electricity and frequency containment reserve markets☆

Nima Mirzaei Alavijeh *, Rahmat Khezri, Mohammadreza Mazidi, David Steen, Le Anh Tuan

Department of Electric Power Engineering, Chalmers University of Technology, 412 96, Gothenburg, Sweden

ARTICLE INFO

Keywords:
Ancillary service
Battery energy storage system
Battery degradation
Frequency containment reserve
Technical market requirements
Revenue stacking

ABSTRACT

This paper presents a novel mixed-integer linear programming (MILP) model for revenue stacking of battery energy storage systems (BESSs) in Sweden's day-ahead (DA) electricity and frequency containment reserve (FCR) markets. The model includes a detailed calendar and cycle battery degradation and market technical requirements modeling that aims to maximize the battery owner's potential profit from participating in the DA and three FCR markets, FCR in normal operation (FCR-N), and FCR in disturbances (FCR-D) for up- and down-regulations. For presenting comprehensive results, successive daily optimizations are conducted for year 2022 using one-minute resolution real data. Five utilization modes are simulated including participation in no FCR market (only DA), only DA and FCR-N, only DA and FCR-D up-regulation, only DA and FCR-D down-regulation, and DA and all FCR markets. The maximum potential profit from revenue stacking in the DA and multi-FCR markets could have been k€ 708 for a 1MW-1MWh BESS, which is 22 times the profit in no FCR participation case. The annual degradation resulting from multi-FCR market participation was 1.7% of loss in battery capacity. Considering degradation in the optimization problem reduced the aging by 29% without a significant effect on profit. The proposed model can serve as a benchmark for evaluating the profitability and sustainability of battery operation strategies and algorithms.

1. Introduction

Frequency containment reserve (FCR) markets are among the market-based tools used by Nordic electricity system operators for regulating grid frequency. FCR services comprise three products: FCR in normal operation (FCR-N) and FCR in disturbances (FCR-D) for up and down regulations, to manage small and larger frequency fluctuations, respectively [1].

Optimizing and analyzing the participation of distributed flexibility resources in FCR markets is increasingly important due to recent market changes. Firstly, in 2022, FCR-D down-regulation market was introduced in the Nordics [2], resulting in three FCR markets and potentially complicating decision-making for flexibility providers. Secondly, the technical requirements for limited energy reservoirs (LERs) have been updated, introducing a maximum available power requirement and reduced endurance requirements in the FCR-D markets [3]. Thirdly, prequalified storage assets in Sweden's FCR markets have increased by 650% from January 2023 to January 2024 [4] indicating strong interest from flexibility asset owners. In the light of these recent developments, revisiting optimal decision-making for the participation of distributed flexibility resources in FCR markets can be valuable for integrating these resources effectively while utilizing their maximum potential. This paper aims to revisit the problem by developing a MILP model to optimize the participation of BESSs in Sweden's day-ahead (DA) and FCR markets. The focus is on finding the maximum potential profit from each market individually and stacked, estimating the expected battery degradation and its impact if considered in the optimization, and incorporating the technical requirements into the MILP problem to generate realistic insights.

☆ The work presented in this paper is financially supported by the following projects: (i) ECom4Future FIWARE Driven Energy Communities for the Future - received funding from the Clean Energy Transition Partnership under Grant Agreement No. CETP22FP-2023-00316, and (ii) Implementation of the Vehicle to Grid Services in Sweden (PAVE) - received funding from Vinnova (Sweden's innovation agency) within the FFI program under the Authority's Dnr 2023-00785.

* Corresponding author.
E-mail address: nima.mirzaei@chalmers.se (N. Mirzaei Alavije).

https://doi.org/10.1016/j.apenergy.2024.125151
Received 21 August 2024; Received in revised form 19 November 2024; Accepted 12 December 2024
Available online 24 December 2024
0306-2619/© 2024 The Authors. Published by Elsevier Ltd. This is an open access article under the CC BY license (http://creativecommons.org/licenses/by/4.0/).

Nomenclature

Acronyms

BESS	Battery energy storage systems
DA	Day-ahead
EV	Electric vehicle
FCR	Frequency containment reserve
FCR-D	Frequency containment reserve in disturbances
FCR-N	Frequency containment reserve in normal operation
LER	Limited energy reservoirs
MILP	Mixed-integer linear programming
OM	Operation and maintenance
SoC	State-of-charge
SoE	State-of-energy

Indices and Sets

Ξ	Set of decision variables
$h \in \mathcal{H}$	Index and set of hours in the day
$t \in \mathcal{T}$	Index and set of time steps in the day

Parameters and Functions

$\Delta p_{t,d}$	Deviation from baseline power due to the activation FCR services [MW]
Δt	The length of the simulation time step [h]
$\eta^{\mathrm{CH}}, \eta^{\mathrm{DS}}$	Charging, discharging efficiency
$\mathcal{A}h_t$	Ah throughput of BESS at time step t of the day [Ah]
$\mathcal{B}^{\mathrm{BAT}}$	Net present value of battery [€]
$\mathcal{B}_t^{\mathrm{CAL}}$, $\mathcal{B}_t^{\mathrm{CYC}}$	Calendar and cycle aging cost of battery degradation on time step t of the day [€]
$\mathcal{C}^{\mathrm{DEG}}$	Cost of battery degradation on the day [€]
$\mathcal{I}_t^c$	C-rate of BESS at time step t of the day
$\mathcal{K}_t$	Temperature at time step t [K]
$\mathcal{S}_t$	State of energy of BESS in time step t of the day [MWh]
$\mathcal{U}_t^{\mathrm{CAL}}$, $\mathcal{U}_t^{\mathrm{CYC}}$	Calendar and cycle aging of BESS on time step t of the day [%]
ρ^{g}	Grid utilization tariff [€/MWh]
ρ_h^{spot}	Day-ahead spot market price at hour h [€/MWh]
ρ^{tax}	Fixed electricity tax [€/MWh]
ρ_h^{X}	Capacity reimbursement price for FCR-X market at hour h, X ∈ {N, DU, DD} [€/MW]
ρ_h^{UR}, ρ_h^{DR}	Up/down regulation prices at hour h [€/MWh]
$\underline{P}$, $\overline{P}$	Minimum and maximum charger power (MW)
$\underline{p}^{\Theta,X}$	Minimum bid size for FCR-X market, X ∈ {N, DU, DD} [MW]
$\underline{S}$, $\overline{S}$	Minimum and maximum state-of-energy
C^{DA}	Cost of BESS in day-ahead spot market on the day [€]
C^{REP}	Cost of operation and maintenance of BESS [€]
C^{REP}	Cost of replacement of battery cells [€]
$e_{t/h}^{\mathrm{DR,X}}$, $e_{t/h}^{\mathrm{UR,X}}$	Energy content: Per unit activated energy for down/up regulation for FCR-X service during t or h [h]
EOL	The percentage of retained capacity at end of life of BESS [%]
F	Total profit of the day [€]
f_n	Nominal grid frequency [Hz]
$f_{\max}^{\mathrm{N/D}}$	Grid frequency for full activation of FCR-N or FCR-D services [Hz]
$f_{\min}^{\mathrm{N/D}}$	Minimum grid frequency for FCR-N or FCR-D activation [Hz]
f_t	Grid frequency at time step t of the day[Hz]
i	Interest rate [%]
L	Life time of BESS [Years]
R^{DA}	Revenue of BESS in day-ahead spot market on the day [€]
R^{FCR}	Revenue from FCR market participation on the day [€]
r^{su}	Ratio of salvage cost to replacement cost
R_h^{X}	Revenue from FCR-X market on hour h of the day, X ∈ {N, DU, DD} [€]

Variables

$b_h^{\mathrm{CH/DS,bl}}$	Binary variable for baseline charge/discharge power of BESS at hour h of the day
b_h^X	Binary variable for participation in FCR-X market at hour h of the day, X ∈ {N, DU, DD}
$b_t^{\mathrm{CH/DS}}$	Binary variable for charge/discharge power of BESS in time step t of the day
$p_h^{\mathrm{CH/DS,bl}}$	Baseline (reference) charge/discharge power of BESS at hour h of the day [MW]
$p_h^{\Theta,\mathrm{X}}$	Power bid on FCR-X market on hour h of the day, X ∈ {N, DU, DD} [MW]
$p_t^{\mathrm{CH/DS}}$	Charge/discharge power of BESS in time step t of the day [MW]
p_t^{DU}, p_t^{DD}	Activated up or down regulation for FCR-D services by BESS in time step t of the day [MW]
p_t^{NU}, p_t^{ND}	Activated up or down regulation for FCR-N service by BESS in time step t of the day [MW]

1.1. Literature review

The literature on BESS applications in frequency regulation services can be divided into two distinct approaches: control-based and market-based. The first approach focuses on the optimal control of BESS to effectively regulate frequency [5–8]. The second approach focuses on investigating the participation of BESS in ancillary service markets, aligning closer with the aim of this study. The literature review is therefore focused on the second approach.

To ensure an acceptable and sustainable operation, it is essential to incorporate technical requirements and analyze the potential degradation of BESSs. The importance of considering battery degradation is highlighted in [9] due to the considerable energy throughput and frequent cycling in FCR-N services. Ref. [10] has analyzed degradation impacts from providing FCR services in Germany based on measurements from a large scale battery. The results indicate that

BESS have been subjected to frequent cycles with low average cycle depth, leading to calendar aging being dominant over cyclic aging. In [11], degradation has been identified as the most critical factor affecting the profitability of BESS. Additionally, the combination of prices and different technical requirements in the three markets further complicates the optimal utilization of flexibility resources. As shown in [9], selecting the best combination of FCRs in each hour of BESS scheduling can increase profitability by 22% compared to delivering only FCR-N. As investigated in [12], overlooking market and technical requirements can lead to underperformance in providing the service and penalties.

In light of the important factors mentioned above, the literature is reviewed with a focus on battery degradation, multi-market decision making, and compliance with technical requirements. Ref. [13] proposes a bidding strategy and an online control methodology for BESS participation in both the electricity day-ahead and FCR-N markets. Although battery degradation is modeled in [13], participation in the FCR-D up/down markets is not considered, and the model is nonlinear, adding a computational burden and challenges in finding the global optimum solution. In [14], a two-stage stochastic optimization model is developed for the optimal bidding of BESS in both the energy and ancillary service markets but the model does not fully account for market requirements and its degradation modeling is simplistic. In [15], a two-level optimization model is proposed to aggregate EVs a BESS for optimal participation in energy and ancillary service markets. However, their model considers only the FCR-N market and overlooks degradation and market requirements. In [16], robust and stochastic methods were used to model the participation of aggregated EVs in energy and ancillary service markets. However, the model was not developed with the technical requirements of Nordic FCR markets, and battery degradation is not a detailed model. Similarly, [17] have introduced an optimization model for the size and scheduling of BESS to maximize income from participating in the energy and FCR-N markets. However, the proposed model has employed a simplified degradation model and has overlooked the requirements of the FCR markets.

Despite extensive studies, there is a lack of research that simultaneously addresses three essential factors in BESS participation in FCR markets: (1) detailed battery degradation modeling, (2) multi-market decision-making, and (3) compliance with technical requirements. Existing research has not fully combined these elements, limiting practical application for optimizing sustainable, complied, and profitable operation strategies for BESS in Nordic FCR markets.

Furthermore, including the three mentioned factors in modeling frequency regulation services faces challenges that existing methods only partially address. Two common modeling approaches are the energy content-based approach and the droop-based power modeling approach. Energy content-based models, such as [9,16,18], use an activation ratio for each timestep, enabling hourly time resolution but simplifying cycle aging by not directly modeling battery charge/discharge power. While this approach removes frequency from the model formulation, it does not capture the specific charge/discharge dynamics critical for accurate aging analysis. The activation ratio represents the frequency variations in the form of a normalized energy-content which can be multiplied by the power bid to represent the equivalent bulk of energy corresponding to the service activation. The activation ratio can be scenario-based [16], an average [18], or based on high-resolution historical frequency values [9]. In contrast, droop-based models, such as [14], accurately represent power fluctuations by linking to droop curves. They are, however, sensitive to time resolution of the model leading to either increased computational complexity when using fine resolutions, or unrealistic representation of power and energy throughput, when using larger time steps.

A novel modeling approach that combines energy content and droop-based methodologies could overcome these limitations. Such a hybrid model would enable detailed battery degradation analysis alongside realistic power and energy throughput, aligning with market technical requirements.

In summary, a comprehensive model that integrates these three key factors – battery degradation, multi-market optimization, and technical requirements – remains absent from the literature. This study seeks to fill this gap by developing a hybrid approach that accurately captures the dynamics of BESS participation in FCR markets while ensuring computational efficiency.

1.2. Approach and contributions

To address the identified gap, this study presents a novel MILP model for multi-market revenue stacking in Sweden's DA and the three FCR markets, incorporating all technical requirements and comprehensive battery degradation modeling. The proposed formulation combines energy content-based and droop-based approaches while enabling the potential stacked hourly participation in the FCR markets and optimizing the purchased power from the DA spot market that acts as an optimal reference power for delivering FCR services and energy recovery. From a practical point of view, the developed model offers flexibility service providers a valuable benchmark to obtain insights into life-time sustainable and profitable operation strategies for BESSs. The main contributions of this study can be summarized as follows:

- Formulating a novel hybrid MILP model for revenue stacking of BESSs in DA spot and multi-FCRs markets, solvable by commonly used optimization solvers.
- Incorporating all Nordic FCR technical requirements and conducting a comprehensive case-study comprising successive daily optimizations for a year using real data of one-minute resolution.
- Applying a detailed model of battery degradation in the developed model to ensure a profitable and sustainable operation.

1.3. Paper organization

The rest of the paper is structured as follows. The frequency containment reserve and market requirements are presented in Section 2. The model formulation considering battery degradation is described in Section 3. The case study and the input data are elaborated in Section 4. The results and discussion are given in Section 5 and conclusions are provided in Section 6.

2. Frequency containment reserves in Sweden

Three FCR markets exist in Sweden: FCR-N, FCR-D up-regulation and FCR-D down-regulation are different from the perspective of regulation and technical requirements. The main aspects of the FCR services are summarized in Table 1. For a realistic model formulation, considering these aspects is essential.

From a market perspective, the difference between the FCR services concerns their remuneration. All three services are remunerated for their cleared bid capacity based on pay-as-cleared prices [19]. The activated energy in FCR-N is also compensated for due to the relatively higher energy throughput in FCR-N services. Up-regulation energy is compensated with up-regulation prices, and down-regulation prices are used to compensate down-regulation energy. The details of the compensation models are provided in the equations of Section 3.1.

According to Sweden's transmission system operator [20], trading for all FCR products is finalized one day (D-1) prior to delivery. Bidding for FCR products is possible in two auctions, both starting seven days before the delivery day with gate closures at 00:30 CET and 18:00 CET on D-1. In the DA spot electricity market, participants submit their bids for the following day before the gate closure at 12:00 CET on D-1. The clearing results are published at 12:42 CET on D-1. Cleared positions in the DA electricity spot market can be used as a reference power or baseline for delivering FCR services, assuming the buyer and sellers of

Table 1
Comparison of market and technical requirements of frequency containment reserve services [3,19].

	FCR-N	FCR-D up	FCR-D down
Market			
Trading time	Day-ahead	Day-ahead	Day-ahead
Remuneration	Capacity and energy	Capacity	Capacity
Min bid size	0.1 MW	0.1 MW	0.1 MW
Technical requirements			
Required power upwards	$1.34 \cdot p_h^{\Theta,N}$	$p_h^{\Theta,DU}$	$0.2 \cdot p_h^{\Theta,DD}$
Required power downwards	$1.34 \cdot p_h^{\Theta,N}$	$0.2 \cdot p_h^{\Theta,DU}$	$p_h^{\Theta,DD}$
Required endurance upwards	1 h	$\frac{1}{3}$ h	0
Required endurance downwards	1 h	0	$\frac{1}{3}$ h
Activation	Automatic (Fig. 1)	Automatic (Fig. 1)	Automatic (Fig. 1)

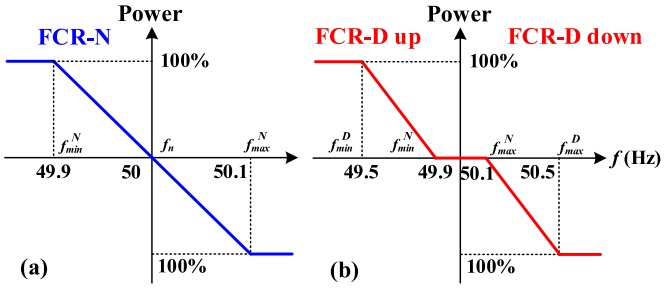

Fig. 1. Frequency containment reserve activation power based on grid frequency: (a) FCR-N, (b) FCR-D.

electricity in DA spot market would like to keep their positions to avoid imbalance penalties. This approach is further explained in Section 3.3.

To calculate a realistic profit, technical requirements from the FCR markets need to be considered. ENTSO-e is the European association for the cooperation of transmission system operators that has provided the technical requirements [3] for limited energy reservoirs (LER) such as EVs and batteries. The power requirements are formulated based on the accepted bid $P_h^{\Theta,X}$. The endurance requirements indicate how long the service provider must be able to provide the accepted bid at a full activation scenario.

The activation of FCR services is based on the specified droop curves shown in Fig. 1. These curves should be strictly followed for the accepted bid size. There are exceptions for LERs in case their state of charge (SOC) goes below or above certain limits specified in [3]. In case these limits are passed, the resource should deviate from the droop curves to bring back the SOC to the acceptable ranges. In such cases, the service provider will not be compensated as it cannot provide the service. These exceptions are not considered in this study, and instead a safety margin is implemented for the SOC by its lower and upper bounds.

Considering the market and technical requirements in the model is essential for a realistic estimation of bidding behavior and profitability of services. In Section 3, a novel MILP formulation is proposed to implement these requirements.

3. Model formulation

The developed optimization model is presented in this section. The model formulation is presented in different subsections that present the objective function and constraints related to the physical limits of the battery, the rules and requirements of participation in FCR, and the battery degradation model.

3.1. Objective function

The objective function of the BESS scheduling problem is to maximize the daily profit given by:

$$f = \max_{\Xi} \quad F \tag{1a}$$

$$= \max_{\Xi} \quad (R^{DA} + R^{FCR} - C^{DA} - C^{DEG})$$

$$\Xi = \{p_h^{CH,bl}, p_h^{DS,bl}, p_t^{CH}, p_t^{DS}, p_h^{\Theta,N}, p_h^{\Theta,DU}, p_h^{\Theta,DD} \mid h \in \mathcal{H}, t \in \mathcal{T}\} \tag{1b}$$

where $\mathcal{T}$ is the set of all the timestamps in the day with a length of lower than one hour, $\mathcal{H}$ is the set of all hours in the day. R^{DA} is the revenue from the DA spot market through discharging, R^{FCR} is the revenue from FCR participation, C^{DA} is the cost in DA spot market through charging, and C^{DEG} is the cost for battery degradation. The decision variables of the optimization problem are the hourly purchased and sold power in the DA spot market ($p_h^{CH,bl}, p_h^{DS,bl}$) that act as the reference point (baseline) for the FCR services, the charging and discharging power of the battery (p_t^{CH}, p_t^{DS}), power bid to participate in FCR-N, FCR-D up and FCR-D down ($p_h^{\Theta,N}$, $p_h^{\Theta,DU}$, $p_h^{\Theta,DD}$).

DA spot market revenue is formulated based on hourly spot market price (ρ_h^{spot}), and discharging power ($p_h^{DS,bl}$).

$$R^{DA} = \sum_{h \in \mathcal{H}} p_h^{DS,bl} \cdot (\rho_h^{spot} + \rho^{tax}) \tag{2}$$

The revenue for multi-market FCR participation contains three parts of revenues for FCR-N, down-regulation FCR-D, and up-regulation FCR-D.

$$R^{FCR} = \sum_{h \in \mathcal{H}} R_h^N + R_h^{DD} + R_h^{DU} \tag{3}$$

The FCR-N revenue includes three terms. The first term is the capacity reimbursement for power bid. The capacity is reimbursed according to the FCR-N market price (ρ_h^N) and the amount of power bid ($p_h^{\Theta,N}$). The second and third terms are the energy compensation for up-regulation and down-regulation during the FCR-N participation. These terms are calculated based on the concept of energy content introduced by [9]. Energy content represents the per unit activated energy for up or down ward regulations within a specific timestep t or a specific hour h. It is precalculated based on the frequency and droop settings. Multiplying energy content ($e_h^{UR/DR,N}$), FCR-N power bid, and up and down regulation prices ($\rho_h^{UR/DR}$) at each hour will provides the hourly energy compensation for FCR-N services

$$R_h^N = p_h^{\Theta,N} \cdot \left(\rho_h^N + \rho_h^{UR} \cdot e_h^{UR,N} - \rho_h^{DR} \cdot e_h^{DR,N}\right), \quad \forall h \tag{4}$$

The revenues for FCR-D down and up are only based on capacity reimbursement according to FCR-D up and down prices and the power bid.

$$R_h^{DD} = \rho_h^{DD}\ p_h^{\Theta,DD}, \quad \forall\ h \tag{5}$$

$$R_h^{DU} = \rho_h^{DU}\ p_h^{\Theta,DU}, \quad \forall\ h \tag{6}$$

The expenditure for charging in the DA spot market is formulated based on the hourly spot price, grid utilization cost (ρ^g), electricity tax (ρ^{tax}), and charging power.

$$C^{DA} = \sum_{h \in \mathcal{H}} p_h^{CH,bl} \left(\rho_h^{spot} + \rho^g + \rho^{tax}\right) \tag{7}$$

The cost of battery degradation is the sum of cycle aging cost ($\mathcal{B}_t^{CYC}$) and calendar aging cost ($\mathcal{B}_t^{CAL}$):

$$C^{DEG} = \sum_{t \in T} \left(\mathcal{B}_t^{CAL} + \mathcal{B}_t^{CYC}\right) \tag{8}$$

3.2. Battery constraints

The battery model contains several constraints related to power and state of energy (SoE) in the optimization model. The charging and discharging power are either zero or between $\underline{P}$ and $\bar{P}$. In fact, the power cannot exceed the charger's maximum power limit at any time. On the other hand, due to low efficiency in low power, the chargers do not allow charging or discharging with a power lower than the minimum limit.

$$p_h^{\mathrm{CH,bl}},\ p_h^{\mathrm{DS,bl}}, P_t^{\mathrm{CH}}, P_t^{\mathrm{DS}} \in \{0\} \cup \left[\underline{P}, \overline{P}\right], \quad \forall h \tag{9}$$

To avoid simultaneous charging and discharge, and to implement (9), binary variables (b_t^{CH}, b_t^{DS}, $b_h^{\mathrm{CH,bl}}$, $b_h^{\mathrm{DS,bl}}$) are considered. The sum of the first pair and the sum of the second of binary variables should be less than or equal to one at their respective timestep.

$$b_t^{\mathrm{CH/DS}} \cdot \underline{P} \le p_t^{\mathrm{CH/DS}} \le b_t^{\mathrm{CH/DS}} \cdot \overline{P}, \quad \forall t \tag{10}$$

$$b_h^{\mathrm{CH/DS,bl}} \cdot \underline{P} \le p_h^{\mathrm{CH/DS,bl}} \le b_h^{\mathrm{CH/DS,bl}} \cdot \overline{P}, \quad \forall h \tag{11}$$

$$b_t^{\mathrm{CH}} + b_t^{\mathrm{DS}} \le 1, \quad \forall t \tag{12}$$

$$b_h^{\mathrm{CH,bl}} + b_h^{\mathrm{DS,bl}} \le 1, \quad \forall h \tag{13}$$

The SoE (S_t) is formulated based on the SoE from the previous timestamp ($S_{t-1,d}$), charging and discharging baseline power, and the up and down regulation energy corresponding to FCR services.

$$\begin{aligned} S_t = S_{t-1} + \left(P_h^{\mathrm{CH,bl}} \cdot \eta^{\mathrm{CH}} - P_h^{\mathrm{DS,bl}}/\eta^{\mathrm{DS}}\right) \cdot \Delta t \\ + P_{h_t}^{\Theta,\mathrm{N}} \cdot \left(e_t^{\mathrm{DR,N}} - e_t^{\mathrm{UR,N}}\right) \\ + P_{h_t}^{\Theta,\mathrm{DD}} \cdot e_t^{\mathrm{DR,DD}} \\ - P_{h_t}^{\Theta,\mathrm{DU}} \cdot e_t^{\mathrm{UR,DU}}, \quad \forall t \end{aligned} \tag{14}$$

$$\underline{S} \le S_t \le \overline{S}, \quad \forall t \tag{15}$$

where η^{CH} and η^{DS} are the charging and discharging efficiencies, and $e_t^{\mathrm{UR/DR,X}}$ is the energy content of up- or down-regulation activation for different FCR markets. Hour h_t represents the corresponding hour to timestamp t.

3.3. FCR participation constraints

Several constraints must be considered to satisfy the technical requirements and physical limitations related to stacked multi-FCR market participation. In addition, several constraints are needed to model the charging and discharging power based on droop curves so that it can be used in the battery degradation model in Section 3.4.

The activated power to deliver the FCR-N service is formulated based on the frequency deviations of the power system. It follows the droop control shown in Fig. 1.

$$p_t^{\mathrm{ND}} = \begin{cases} p_h^{\Theta,\mathrm{N}}, & f_t > f_{\max}^{\mathrm{N}} \\ p_h^{\Theta,\mathrm{N}} \left(\frac{f_t - f_n}{f_{\max}^{\mathrm{N}} - f_n}\right), & f_n \le f_t \le f_{\max}^{\mathrm{N}} \\ 0, & f_t < f_n, \end{cases} \quad \forall t, \tag{16}$$

$$p_t^{\mathrm{NU}} = \begin{cases} 0, & f_t > f_n \\ p_h^{\Theta,\mathrm{N}} \left(\frac{f_t - f_n}{f_{\min}^{\mathrm{N}} - f_n}\right), & f_{\min}^{\mathrm{N}} \le f_t \le f_n \\ p_h^{\Theta,\mathrm{N}}, & f_t < f_{\min}^{\mathrm{N}}, \end{cases} \quad \forall t, \tag{17}$$

where f_t is the measured frequency of the system in Hz in timestamp t, f_n is the nominal frequency (50 Hz), $f_{\max}^{\mathrm{N}}$ and $f_{\min}^{\mathrm{N}}$ are the maximum and minimum ranges of frequency for FCR-N participation, 50.1 Hz and 49.9 Hz, respectively.

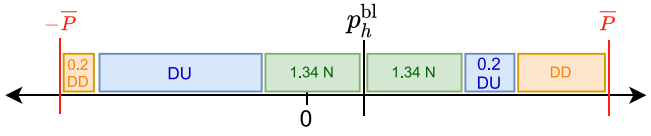

Fig. 2. Limits on frequency containment reserve capacity bids considering the baseline and ENTSOe requirements on power. N: $P_h^{\Theta,\mathrm{N}}$, DU: $P_h^{\Theta,\mathrm{DU}}$, DD: $P_h^{\Theta,\mathrm{DD}}$.

The activated power for delivering FCR-D markets is also formulated based on the frequency deviations of the power system according to Fig. 1.

$$p_t^{\mathrm{DD}} = \begin{cases} p_h^{\Theta,\mathrm{DD}}, & f_t > f_{\max}^{\mathrm{D}} \\ p_h^{\Theta,\mathrm{DD}} \left(\frac{f_t - f_{\max}^{\mathrm{N}}}{f_{\max}^{\mathrm{D}} - f_{\max}^{\mathrm{N}}}\right), & f_{max}^{\mathrm{N}} \le f_t \le f_{\max}^{\mathrm{D}} \\ 0, & f_t < f_{\max}^{\mathrm{N}}, \end{cases} \quad \forall t, \tag{18}$$

$$p_t^{\mathrm{DU}} = \begin{cases} 0, & f_t > f_{\min}^{\mathrm{N}} \\ p_h^{\Theta,\mathrm{DU}} \left(\frac{f_t - f_{\min}^{\mathrm{N}}}{f_{\min}^{\mathrm{D}} - f_{\min}^{\mathrm{N}}}\right), & f_{\min}^{\mathrm{D}} \le f_t \le f_{\min}^{\mathrm{N}} \\ p_h^{\Theta,\mathrm{DU}}, & f_t < f_{\min}^{\mathrm{D}}, \end{cases} \quad \forall t, \tag{19}$$

where $f_{\max}^{\mathrm{D}}$ and $f_{\min}^{\mathrm{D}}$ are the maximum and minimum ranges of frequency for FCR-D participation, 50.5 Hz and 49.5 Hz, respectively.

The activated power for FCR services should be delivered with respect to the original plan of the battery. This is shown in (20) where the original plan is the baseline power. The baseline is the traded energy in the DA spot market in the context of this model. The deviation from the baseline is shown by Δp_t. A positive Δp_t corresponds to down-regulation and negative to up-regulation because load convention is used for the power.

$$\begin{aligned} \Delta p_t &= p_t - p_{h_t}^{\mathrm{bl}} \\ &= \left(p_t^{\mathrm{CH}} - p_t^{\mathrm{DS}}\right) - \left(p_{h_t}^{\mathrm{CH,bl}} - p_{h_t}^{\mathrm{DS,bl}}\right), \quad \forall t \end{aligned} \tag{20}$$

When bidding in the FCR markets, Δp_t should be strictly equal to the specified power levels from the droop controls:

$$\Delta P_t = P_t^{\mathrm{ND}} + P_t^{\mathrm{DD}} - P_t^{\mathrm{NU}} - P_t^{\mathrm{DU}}, \quad \forall t. \tag{21}$$

The lower and upper bounds related to the bids need to be defined. Power bids for each market should not exceed double the maximum power of the battery. The upper bound is double the maximum power because the battery can, for example, go from full charge to full discharge power. The minimum power is also considered for each market participation ($\underline{p}^{\Theta,\mathrm{N}}$, $\underline{p}^{\Theta,\mathrm{DU}}$, and $\underline{p}^{\Theta,\mathrm{DD}}$). Binary variables ($b_t^{\mathrm{N}}$, b_t^{DD}, and b_t^{DU}) are added to implement the minimum power bid:

$$b_h^{\mathrm{N}} \cdot \underline{p}^{\Theta,\mathrm{N}} \le p_h^{\Theta,\mathrm{N}} \le b_h^{\mathrm{N}} \cdot \overline{P}, \quad \forall h, \tag{22}$$

$$b_h^{\mathrm{DD}} \cdot \underline{p}^{\Theta,\mathrm{DD}} \le p_h^{\Theta,\mathrm{DD}} \le b_h^{\mathrm{DD}} \cdot 2\overline{P}, \quad \forall h, \tag{23}$$

$$b_h^{\mathrm{DU}} \cdot \underline{p}^{\Theta,\mathrm{DU}} \le p_h^{\Theta,\mathrm{DU}} \le b_h^{\mathrm{DU}} \cdot 2\overline{P}, \quad \forall h. \tag{24}$$

To have results closer to real life, technical requirements for the FCR markets (Table 1) need to be considered. The power requirements are transferred to the physical limitations of the battery in Fig. 2 using the maximum charge and discharge capacity ($\overline{P}$) and the baseline (p_h^{bl}) which is the reference point for providing the up- or down-regulation. The figure can be formulated as constraints provided in (25) and (26).

$$1.34 p_h^{\Theta,\mathrm{N}} + p_h^{\Theta,\mathrm{DU}} + 0.2 p_h^{\Theta,\mathrm{DD}} \le \overline{P} + p_h^{\mathrm{bl}}, \quad \forall h \tag{25}$$

$$1.34 p_h^{\Theta,\mathrm{N}} + p_h^{\Theta,\mathrm{DD}} + 0.2 p_h^{\Theta,\mathrm{DU}} \le \overline{P} - p_h^{\mathrm{bl}}, \quad \forall h \tag{26}$$

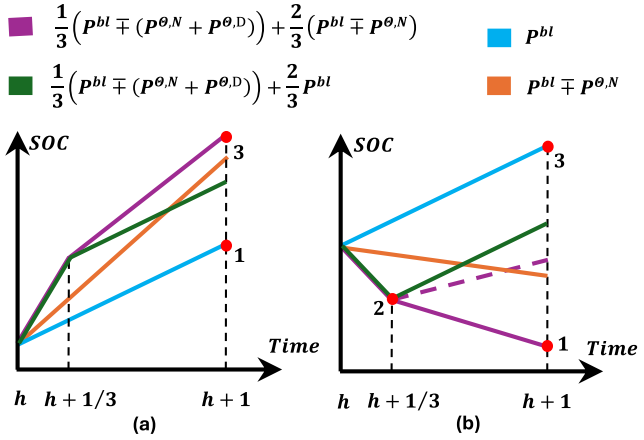

Fig. 3. Examples of critical activation cases for endurance requirement when reference power is at charging. (a) downwards regulation, (b) upwards regulation.

The energy requirements (i.e., endurance) can be implemented for the worst-case scenarios for SoC at each hour. The potential extreme scenarios are visualized in Fig. 3 for up- and downwards activation when the reference power is at charging. A similar analysis can be done for a reference power at discharging. These most critical points are marked with red circles and can occur in the following scenarios:

1. If the service is not activated at all and the battery is locked to follow its baseline: Eq. (27)
2. If both FCR-N and FCR-D services are activated for 20 min: Eq. (28)
3. If FCR-N and FCR-D services are simultaneously activated for 20 min and FCR-N for the remaining 40 min within the hour: Eq. (29)

$$\underline{S} \le S_{h-\Delta t} + P_h^{\mathrm{bl}} \le \overline{S}, \quad \forall h \tag{27}$$

$$\underline{S} \le S_{h-\Delta t} + \left(p_h^{\mathrm{bl}} + p_h^{\Theta,\mathrm{N}} + p_h^{\Theta,\mathrm{DD}}\right) \cdot \frac{1}{3} \le \overline{S}, \quad \forall h \tag{28a}$$

$$\underline{S} \le S_{h-\Delta t} + \left(p_h^{\mathrm{bl}} - p_h^{\Theta,\mathrm{N}} - p_h^{\Theta,\mathrm{DU}}\right) \cdot \frac{1}{3} \le \overline{S}, \quad \forall h \tag{28b}$$

$$\underline{S} \le S_{h-\Delta t} + p_h^{\mathrm{bl}} + p_h^{\Theta,\mathrm{N}} + \frac{1}{3} \cdot p_h^{\Theta,\mathrm{DD}} \le \overline{S}, \quad \forall h \tag{29a}$$

$$\underline{S} \le S_{h-\Delta t} + p_h^{\mathrm{bl}} - p_h^{\Theta,\mathrm{N}} - \frac{1}{3} \cdot p_h^{\Theta,\mathrm{DU}} \le \overline{S}, \quad \forall h \tag{29b}$$

3.4. Battery degradation

The costs of cycle aging and calendar aging of the battery are calculated based on the degradation of the battery due to cycle aging ($\mathcal{U}_{t,d}^{\mathrm{CYC}}$) and calendar aging ($\mathcal{U}_{t,d}^{\mathrm{CAL}}$), percentage of retained capacity at end-of-life (EOL), and the net present value of the battery ($\mathcal{B}^{\mathrm{BAT}}$).

$$\mathcal{B}_t^{\mathrm{CAL}} = \mathcal{B}^{\mathrm{BAT}} \frac{\mathcal{U}_t^{\mathrm{CAL}}(\%)}{100\% - \mathrm{EOL}(\%)}, \quad \forall\, t, \tag{30}$$

$$\mathcal{B}_t^{\mathrm{CYC}} = \mathcal{B}^{\mathrm{BAT}} \frac{\mathcal{U}_{t,d}^{\mathrm{CYC}}(\%)}{100\% - \mathrm{EOL}(\%)}, \quad \forall\, t. \tag{31}$$

Typically, the percentage of retained capacity at the EOL of the battery is considered as 80% [21]. The net present value of the battery is calculated based on the reference average lifetime of the battery (L), interest rate (i), cost of replacement (C^{REP}), cost of operation and maintenance (C^{OM}), and the ratio of salvage cost to replacement cost (r^{SV}). The battery aging needs to be in monetary values so that it can be included in objective function. The net present value is required to transform battery aging to monetary values from empirical degradation formulations that are as percentage of capacity loss.

$$\mathcal{B}^{\mathrm{BAT}} = (1 - r^{\mathrm{SV}})\ C^{\mathrm{REP}} \frac{1}{(1+i)^L} + C^{\mathrm{OM}} \frac{(1+i)^L - 1}{\alpha\,(1+i)^L} \tag{32}$$

The battery degradation model is taken from [22] where an experimental model was developed for a Lithium-Nickel-Manganese-Cobalt + Lithium-Manganese oxide battery. The authors derived nonlinear empirical aging models for the same battery in which calendar aging depends on SOC, temperature ($\mathcal{K}_t$), and battery age in days ($\mathcal{Q}$), and the cycle aging depends on temperature, C-rate ($\mathcal{I}_t^c$), and Ah-throughput ($\mathcal{A}h_t$).

$$\mathcal{U}_t^{\mathrm{CAL}} = \mathcal{F}\left(S_t, \mathcal{K}_t, \mathcal{Q}\right), \quad \forall t \tag{33}$$

$$\mathcal{U}_t^{\mathrm{CYC}} = \mathcal{F}\left(\mathcal{K}_t, \mathcal{I}_t^c, \mathcal{A}h_t\right), \quad \forall t. \tag{34}$$

The model of calendar aging is a nonlinear function:

$$\mathcal{U}_t^{\mathrm{CAL}} = G\left(S_t\right)\ e^{\left(\frac{E_a}{R\,\mathcal{K}_t}\right)} \mathcal{Q}^{0.5}, \quad \forall t, \tag{35}$$

$$G\left(S_t\right) = \begin{cases} a_1 {S_t}^2 + a_2 S_t + a_3, & 0 \le S_t \le 0.5Q \\ b_1 {S_t}^2 + b_2 S_t + b_3, & 0.5Q < S_t \le 0.7Q \\ c_1 {S_t}^2 + c_2 S_t + c_3, & 0.7Q < S_t \le 1.0Q, \end{cases} \quad \forall t. \tag{36}$$

Eq. (35) is included in the problem by piece-wise linearization using binaries and auxiliary variables over the three SoC spans in (36).

The cycle aging model [22] is also non-linear:

$$\mathcal{U}_t^{\mathrm{CYC}} = \left(q_1 {\mathcal{K}_t}^2 + q_2 \mathcal{K}_t + q_3\right) e^{q_4 \mathcal{I}_t^c}\, \mathcal{A}h_t, \quad \forall t. \tag{37}$$

The cycle aging is linearized over the operation range of the battery as given in Table 2, and assuming a relatively constant temperature of 20 °C because stationary batteries are commonly kept in containers with regulated temperatures and effective battery management systems.

Detail of mathematical linearization for calendar aging and cycle aging models is presented in [21] and in Appendix. The aging parameters used are presented in Table 2.

4. Simulated cases and input data

The impact of degradation is assessed for five market participation cases:

- Case w/o FCR: without any FCR participation,
- Case FCR-N: participate only in FCR-N,
- Case FCR-DU: participate only in FCR-D up,
- Case FCR-DD: participate only in FCR-D down,
- Case multi: multi-market participation is allowed at every hour.

The five cases are run twice, once when the degradation cost is included in the objective function and once without the degradation cost. For the latter, the degradation cost is post-calculated and included in calculating the profit. Successive daily optimizations are run for a complete year using a timestep of one minute. This means that the length of $\mathcal{H}$ is 24 h and the length of $\mathcal{T}$ is 24 × 60 in each optimization problem.

4.1. Comparison metrics

The results are evaluated from two perspectives: monetary, and operation strategy. The monetary perspective compares the cases based on profit and degradation costs. The operation strategy compares the distribution of SoE, baseline power, and bid size, in addition to the number of hours to participate in different combinations of markets.

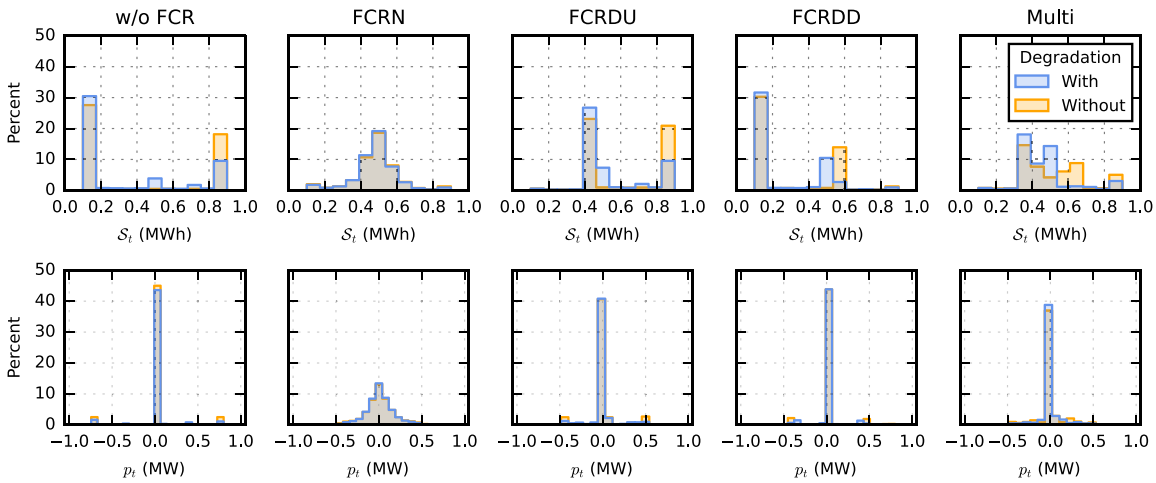

Fig. 4. The battery utilization in different cases visualized by the histogram of battery SoE (S_t) and power (p_t) as a percentage of all time step in a year.

Table 2
Battery input parameters.

Parameter	Value	Parameter	Value
SoC range	10%–90%	Battery capacity	1 MWh
Dis/Charge efficiency	93%	Min, max dis/charge power	0.0 MW, 1.0 MW
Battery OM cost	2% · 137 k€/MWh	Battery replacement cost	137 k€/MWh
EOL	80%	Interest rate	5%
Reference average lifetime	10 years	Ratio of salvage cost	0.5
Temperature	20° C		
Cycle aging parameters [22]			
At 20 °C: $q_1\mathcal{K}_t^2 + q_2\mathcal{K}_t + q_3 = 0.0008,\ q4 = 0.3903$			
Calendar aging parameters [22,26]			
$E_a = 24.5$ kJ mol^{-1}, $R = 8.314$ J mol^{-1} K^{-1}, $a_1 = -1.1$, $a_2 = 89.7$, $a_3 = 1224.6$, $b_1 = 10.3$, $b_2 = -1083.6$, $b_3 = 31\,447$, $c_1 = 2.6$, $c_2 = -409.5$, $c_3 = 22\,035$			

4.2. Input data

The input data consists of the input parameters for the battery whose degradation model was formulated and the market-related data including frequency data and prices for the DA market, FCR-N, FCR-D up, FCR-D down, and imbalance. Battery input parameters are provided in Table 2, the battery data are taken from [21], prices are taken from [23,24], and frequency data is taken from [25]. Market zone SE3 and the year 2022 are used for prices and frequency data.

5. Results and discussion

Monetary results are presented in Table 3. Profit for cases without considering battery aging cost in the objective function is obtained by post-calculating the aging cost and subtracting it from the objective function values. For the cases with considering aging cost, the objective function and profit values are equivalent because the degradation cost is included in the objective function. However, for the cases without degradation cost, the profit cost would be lower than the objective function as the profit value is equivalent to objective function minus degradation cost. The results show that the multi-market case has a significantly larger profit compared to other market participation cases while having the second smallest degradation cost. Another observation is that considering degradation in optimization does not have a considerable impact (≤1%) on the profit except in case w/o FCR. However, the total annual aging cost has been reduced by 5%–29% when battery degradation is considered in the optimization. This highlights that considering degradation in the objective function can provide operation strategies that not only result in a similar profit but also a longer lifetime for the battery. The utilization of the battery is visualized in Fig. 4 for clarifying the reduction of battery degradation. The SoE and power data points show a shift towards smaller absolute values when degradation is considered. This explains the reduction of the aging costs when degradation is considered in the optimization.

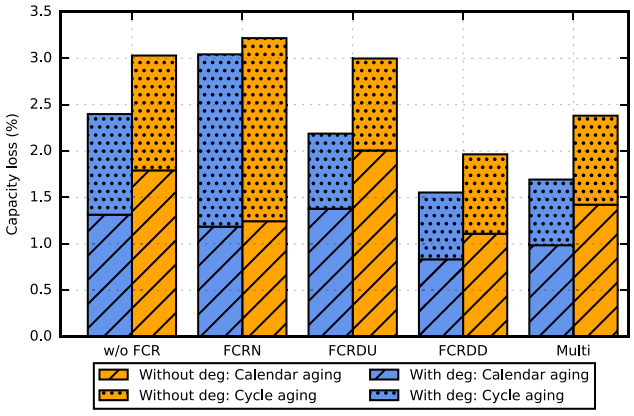

Fig. 5. The annual battery capacity loss due to calendar and cycle aging for the different market participation cases.

The total capacity loss of the battery over the year, $\sum_d \sum_t \mathcal{U}_{t,d}(\%)$, is presented in Fig. 5. The largest degradation is expected in the FCR-N cases while the lowest degradation is expected for the FCR-D down cases. This is due to the large energy throughput and cycling for FCR-N cases while the FCR-D down cases require both lower cycling and SoC levels. In addition, FCR-N cases have the largest cycle aging costs while FCR-D up cases show the largest calendar aging. It is also worth noting that the multi-market participation cases have shown a lower

Table 3
Annual monetary results in k€.

Case	W/o aging in objective function			With aging in objective function			Δ Profit	Δ Aging cost
	Profit (including aging)	Objective function	Aging cost	Profit (including aging)	Objective function	Aging cost		
w/o FCR	30.8	40.4	9.6	31.9	31.9	7.6	3.6%	−21%
FCR-N	213.2	223.4	10.2	214.3	214.3	9.6	0.5%	−5%
FCR-DU	559.7	569.2	9.5	561.2	561.2	6.9	0.3%	−27%
FCR-DD	302.6	308.8	6.2	302.6	302.6	4.9	0.0%	−21%
Multi	706.1	713.6	7.5	707.9	707.9	5.4	0.3%	−29%

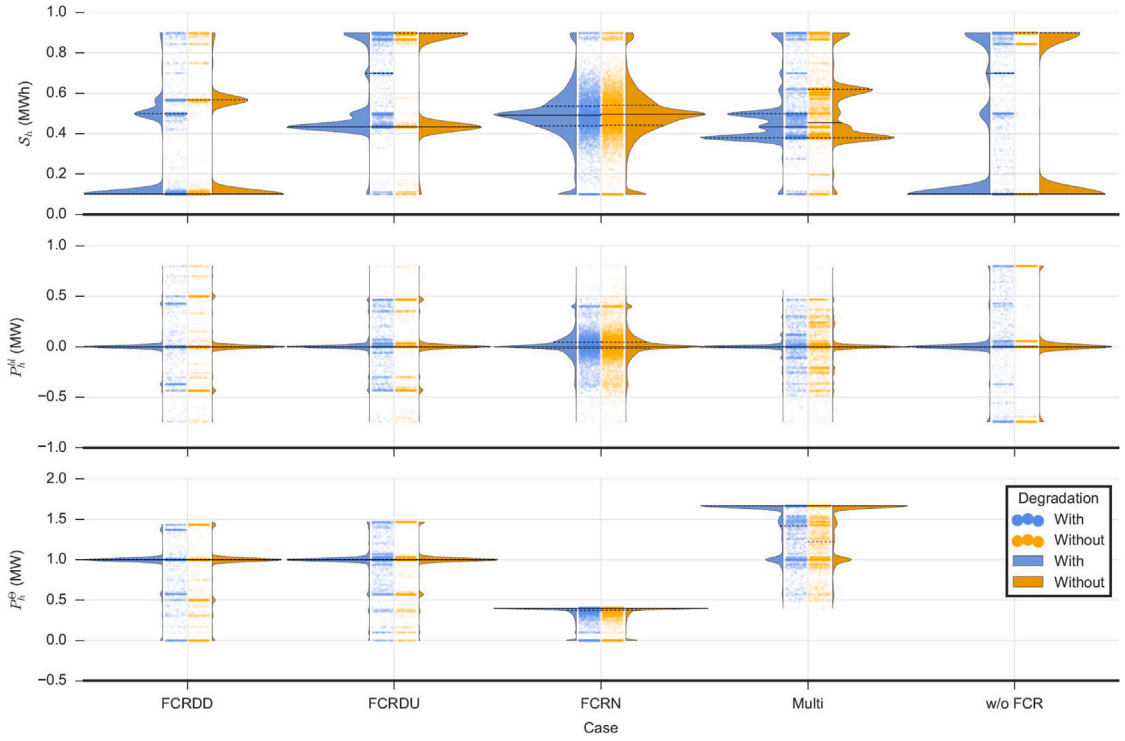

Fig. 6. Operation strategy including the distribution of state of energy at the beginning of each hour (S_h), baseline power(p_h^{bl}), and bid size (p_h^{Θ}) for the simulated cases.

degradation compared to the w/o FCR because the battery is utilized at lower SoC and power setpoints.

To better understand the difference in the operation strategies, the distribution of SoE in the beginning of each hour (S_h), baseline power (p_h^{bl}), and bid size (p^{Θ}) are presented in Fig. 6. The dashed lines show the first, second, and third quartiles. SoE at the beginning of each hour is considered as a part of the strategy because it is one of the main variables for satisfying the endurance requirements. For multi-market cases, the sum of bids in all the FCR markets is presented in Fig. 6.

Several general observations can be made regarding the most dominant values for the strategy variables presented in Fig. 6. SoE at the beginning of each hour (S_h) seems less discrete in the FCR-N case compared to the other cases. The dominant baseline power for all the cases is zero MW while the FCR-N case shows again a less discrete distribution. These two observations can highlight the potential complexities of real-life planning of an optimal FCR-N strategy compared to the other market participation cases which most likely boils down to the large energy throughput and a more regular activation of FCR-N services.

The dominant bid sizes for cases FCR-D up and FCR-D down is 1 MW (Fig. 6). The larger bids were possible at hours with a non-zero reference power. The bids in the FCR-N case are limited to 0.4 MW due to considering technical requirements and the battery capacity. FCR-N is a symmetrical service with a required 1 h endurance. Therefore, for example, if the SoE is at 0.5 MWh, only 0.4 MW can be provided for 1 h in each direction considering the allowed SoC range as given in Table 2. For case Multi, the sum of the bids in all FCR markets are presented showing a dominant sum at 1.6 MW. This is the dominant optimal bidding strategy which is a simultaneous bid in FCR-D up and down markets (Table 4). The sum is limited to 1.6 MW because of the technical requirement of power indicating a 20% power availability in the opposite direction. The bid size results are yet another observation regarding the impact of considering technical requirements and their importance in obtaining realistic bidding and operation strategies.

The operation strategies can be further analyzed using the relation between the variables including SoE, baseline power, and bid size. Fig. 7 shows the heatmap and the conjunction between these variables for the FCR cases considering degradation. An outer parallelogram is distinctly visible in all subfigures that its four sides represent the physical limits of the battery, i.e., power and energy capacity. The visible lines formed inside the parallelogram are mostly due to the technical requirements for FCR markets in combination with the physical limits of the battery. For example, in the FCR-N subfigure, the red line in the middle represents the maximum potential bid in FCR-N, 0.4 MW, due to the requirements for symmetrical up- and down-regulation and the 1 h endurance in both up- and down-regulation directions. If S_h is at 0.9 MWh, the baseline power p_h^{bl} should be at −0.4 MW to allow for a 1 h long full activation of the 0.4 MW bid p_h^{Θ} for up or down regulation and not violating the upper and lower bounds of S_h. Following the red line to lower S_h values, p_h^{bl} needs to increase to allow for a 0.4 MW bid while satisfying the mentioned requirements. Another example of technical requirements can be found in the FCR-DU subfigure. The

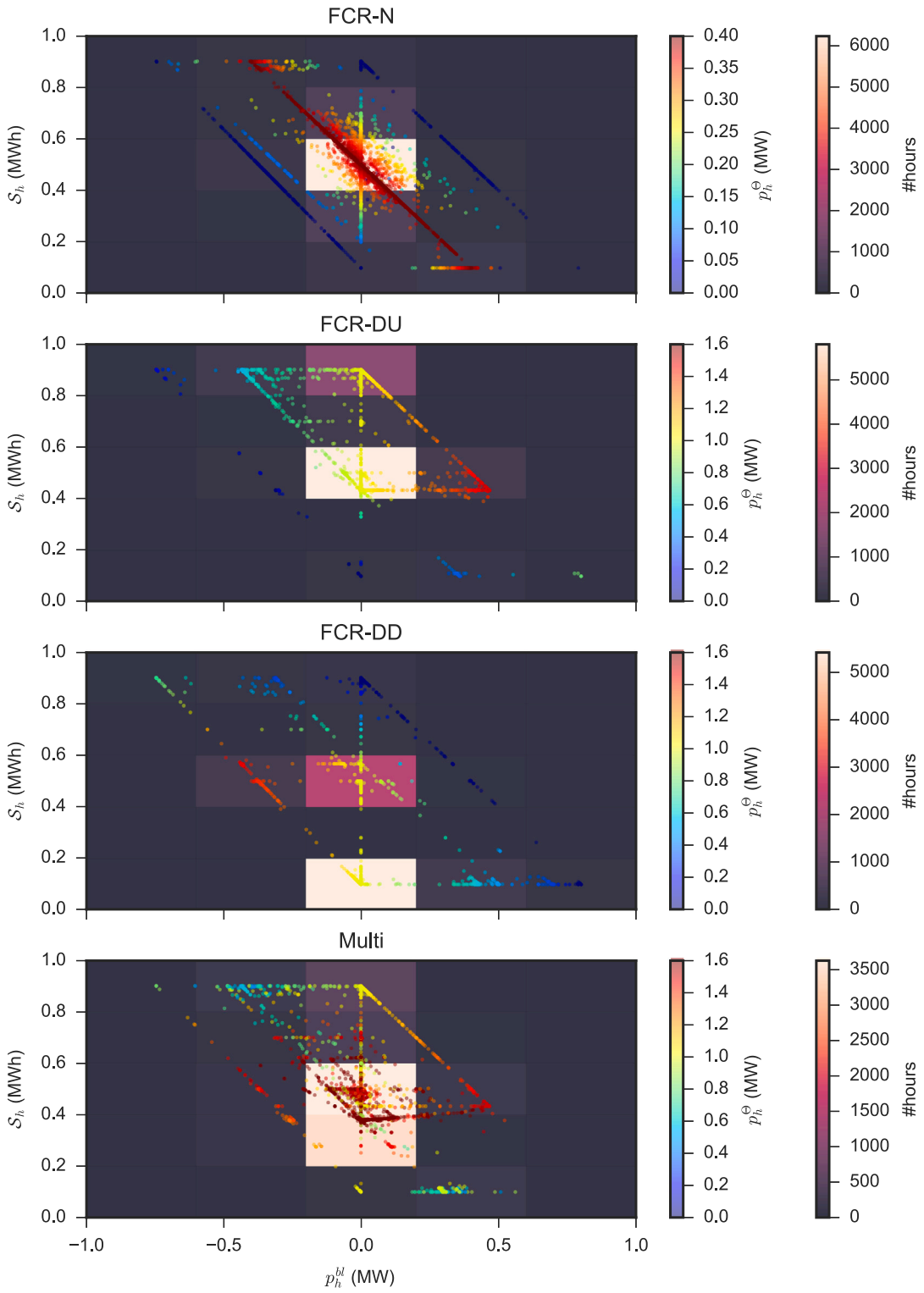

Fig. 7. The heatmap of operation strategy variables, state of energy at the beginning of each hour (S_h), baseline power (p_h^{bl}), and bid size (p_h^{Θ}), for the cases considering degradation.

inner horizontal line right above $S_h = 0.4$ MWh is directly connected to the required endurance of 20 min for FCR-D up regulation. A full-activation of $p_h^{\Theta} = 1$ MW for 20 min and with a $p_h^{bl} = 0$, leads to a 0.33 MWh reduction in S_h where we hit the lower bound of S_h at 0.1 MWh. Therefore, for a larger p_h^{Θ} at $S_h = 0.43$ MWh, a larger p_h^{bl} is required, moving along the horizontal line to the right. In the multi-FCR subfigure, the technical requirements cannot be seen as distinct as in other cases that is due to the mixture of different markets at different hours. However, it can be seen that the number of zero bids, the dots in blue, has been significantly reduced compared to other cases. This can also be seen in Table 4 under column None. This shows how combining different markets could benefit the battery owner by increasing the market participation and profit.

The mix of chosen markets in each case is presented in Table 4. The inclusion of degradation in the objective function has led to a larger number of market participation hours. This is because the BESS can

Table 4
Choice of market as the number of hours in a year. Market choices include N: FCR-N; DU: FCR-D up-regulation; DD: FCR-D down-regulation; N+DU: FCR-N and FCR-D up; N+DD: FCR-N and FCR-D down; DU+DD: FCR-D up and down; All: FCR-N, FCR-D up and FCR-D down.

Case	None	N	DU	DD	N+DU	N+DD	DU+DD	All
	Without aging in objective function							
w/o FCR	8760	–	–	–	–	–	–	–
FCR-N	892	7868	–	–	–	–	–	–
FCR-DU	73	–	8687	–	–	–	–	–
FCR-DD	279	–	–	8481	–	–	–	–
Multi	0	3	1741	145	164	76	6110	521
	With aging in objective function							
w/o FCR	8760	–	–	–	–	–	–	–
FCR-N	715	8045	–	–	–	–	–	–
FCR-DU	70	–	8690	–	–	–	–	–
FCR-DD	202	–	–	8558	–	–	–	–
Multi	0	2	1540	147	93	75	6382	521

reduce calendar aging by regulating SoC. The change in the strategy comprises a larger number of participation hours but with a reduction in the number of hours that have the largest bidding power. This effect can be seen more clearly for the largest bids in cases FCR-D down and FCR-D up presented in Fig. 6. The dominant bid combination for case Multi is simultaneous FCR-DU and FCR-DD participation. This dominant bid combination besides the SoE levels in Fig. 4 can clarify why the total battery degradation in Multi case is between the FCR-D up and FCR-D down cases (Fig. 5).

It is worth noting that the model should not be seen as a bidding algorithm. The presented profit values are the theoretical maximum profit given the perspective of an oracle. In real-life, these profits might not be achieved to their full extent due to the lack of information and uncertainties in the input parameters. However, the model and its results can be interpreted as a benchmark indicating the maximum potential profit, and the potential impact of considering battery degradation in the optimization. Hence, the model can be used as an oracle model to evaluate and compare real-life bidding models that takes into account uncertainties in input parameters.

Furthermore, the presented monetary values and strategies depend on market prices and the battery size. Therefore, the results presented can vary if the battery power and energy capacity are changed or simulations are run for another year. A battery sizing study to find the optimal power-to-energy ratio for FCR market participation can be a future work, especially given the impact of the technical requirements.

6. Conclusions

In this study, a novel MILP formulation was presented for participation in Sweden's DA and its three FCR markets while including a detailed cycle and calendar aging in addition to the most recent technical requirements. Successive daily optimizations were run for a full-year case study in 2022 to find the maximum potential profit from individual and stacked participation in these markets in addition to the expected calendar and cycle aging. The impact of considering degradation and technical requirements was also discussed.

The results showed that the maximum profit could have been achieved in the multi-market participation that was dominated by simultaneous bidding in FCR-D up and down markets. The maximum potential profit was k€708 with an expected degradation of 1.7% battery capacity loss. The largest degradation was expected from the dedicated FCR-N participation case with 3.0% battery capacity loss, while the lowest degradation was shown to be for the dedicated FCR-D down participation case with 1.6% capacity loss. In addition, the results showed that, except for the case w/o FCR, considering degradation in the optimization does not have a significant impact on profits while it can decrease the aging by 5%–29% leading to a more sustainable battery operation. The results have also clearly demonstrated the impact and importance of fulfilling the technical requirements of the Nordic FCR markets.

The proposed model and the results can be utilized by flexibility asset owners to obtain more sustainable and yet profitable operation strategies. In addition, the formulation can be seen as an oracle model providing a maximum potential profit. This can be utilized as a benchmark for evaluating bidding models considering uncertainties.

CRediT authorship contribution statement

Nima Mirzaei Alavijeh: Writing – original draft, Visualization, Software, Methodology, Formal analysis, Conceptualization. **Rahmat Khezri:** Writing – review & editing, Methodology, Conceptualization. **Mohammadreza Mazidi:** Writing – original draft, Methodology, Formal analysis, Conceptualization. **David Steen:** Writing – review & editing, Supervision, Methodology, Funding acquisition, Formal analysis, Conceptualization. **Le Anh Tuan:** Writing – review & editing, Supervision, Funding acquisition, Conceptualization.

Declaration of Generative AI and AI-assisted technologies in the writing process

During the preparation of this work, the authors used ChatGPT to enhance readability and language. After using this tool/service, the authors reviewed and edited the content as needed and take full responsibility for the content of the publication.

Declaration of competing interest

The authors declare that they have no known competing financial interests or personal relationships that could have appeared to influence the work reported in this paper.

Appendix. Battery aging linearization

In this section, details of model linearization are provided for cycle and calendar aging formulations.

The nonlinear term $G(S_t)$ in calendar aging formulation (35) is fitted with a piecewise function of state-of-charge as shown in (36). As in [21], piecewise linear approximation method is used to linearize (36) into (A.1).

$$G\left(S_t\right)=\begin{cases}\alpha_1 S_t+\alpha_2 & 0\le S_t\le 0.5Q\\ \beta_1 S_t+\beta_2 & 0.5Q< S_t\le 0.7Q\\ \gamma_1 S_t+\gamma_2 & 0.7Q< S_t\le 1.0Q,\end{cases}\quad \forall t. \tag{A.1}$$

Eq. (A.1) is a three-condition constraint which is transformed into (A.2a) using three binary variables χ_t, ψ_t, ω_t, additional constraints (A.2b), (A.2c), (A.2d). The coefficients are presented in Table A.5.

$$G(S_t)=(\alpha_1 S_t+\alpha_2)\chi_t+(\beta_1 S_t+\beta_2)\psi_t+(\gamma_1 S_t+\gamma_2)\omega_t,\quad \forall t \tag{A.2a}$$

$$\chi_t+\psi_t+\omega_t=1,\quad \forall t \tag{A.2b}$$

$$S_t\ge 0.5Q\psi_t-M_1\chi_t+0.7Q\omega_t,\quad \forall t \tag{A.2c}$$

$$S_t\le 0.5Q\chi_t+0.7Q\psi_t+M_2\omega_t,\quad \forall t \tag{A.2d}$$

In (A.2a), the product of continuous variable S_t and the binary variables χ_t, ψ_t, and ω_t creates nonlinear terms. These are replaced by three continuous variables X_t, Ψ_t, and Ω_t to linearize the equation as follows:

$$G(S_t)=\alpha_1 X_t+\alpha_2\chi_t+\beta_1\Psi_t+\beta_2\psi_t+\gamma_1\Omega_t+\gamma_2\omega_t \tag{A.3a}$$

$$0\le X_t\le M_3\chi_t \tag{A.3b}$$

$$S_t-M_3(1-\chi_t)\le X_t\le S_t \tag{A.3c}$$

Table A.5
Calendar and cycle aging linearization parameters.

Parameters	Values	Parameters	Values
α_1	36.7	α_2	1224.6
β_1	168.7	β_2	3103.7
γ_1	41.9	γ_2	6265.2
ν_1	2.216	ν_2	0

$$0 \le \Psi_t \le M_4 \psi_t \tag{A.3d}$$

$$S_t - M_4(1-\psi_t) \le \Psi_t \le S_t \tag{A.3e}$$

$$0 \le \Omega_t \le M_5 \omega_t \tag{A.3f}$$

$$S_t - M_5(1-\omega_t) \le \Omega_t \le S_t \tag{A.3g}$$

In the cycle aging model (37), the nonlinear term is the exponential function $e^{q_4 I_t^c}$, where I_t^c is the C-rate. C-rate can be calculated using (A.4) where Q_0 is the battery capacity, and I_t is the current of the battery pack. Using C-rate, the exponential term can be rewritten as in (A.5).

$$I_t^c = \frac{I_t}{Q_0} = \frac{p_t^{\mathrm{CH}}\eta^{\mathrm{CH}} + \frac{p_t^{\mathrm{DS}}}{\eta^{\mathrm{DS}}}}{Q_0} \tag{A.4}$$

$$e^{q_4 I_t^c} = e^{\frac{q_4}{Q_0}\left(p_t^{\mathrm{CH}}\eta^{\mathrm{CH}} + \frac{p_t^{\mathrm{DS}}}{\eta^{\mathrm{DS}}}\right)} = e^{q_5 \mu_t} \tag{A.5}$$

To estimate Ah_t in (37), the cumulative charge is used as follows:

$$\mathrm{Ah}_t = I_{\mathrm{cell},t}\Delta t = \frac{\left(p_t^{\mathrm{CH}}\eta^{\mathrm{CH}} + \frac{p_t^{\mathrm{DS}}}{\eta^{\mathrm{DS}}}\right)}{n_c V_c}\Delta t = \frac{\mu_t}{n_c V_c}\Delta t = \frac{\mu_t Q_c}{Q_0}\Delta t, \tag{A.6}$$

where n_c is the number of cells, V_c is the nominal cell voltage, and Q_c is the nominal cell capacity. Q_c is 1.5 Ah [22]. Cycle aging (37) can be rewritten as follows:

$$\mathcal{U}_t^{\mathrm{CYC}} = (q_1 \mathcal{K}_t^{\,2} + q_2 \mathcal{K}_t + q_3)(e^{q_5 \mu_t})\left(\frac{\mu_t Q_c}{Q_0}\Delta t\right) \tag{A.7}$$

Since μ_t is constrained within the specific operating range of the battery, a linear approximation is applied for linearization:

$$\mathcal{U}_t^{\mathrm{CYC}} = (q_1 \mathcal{K}_t^{\,2} + q_2 \mathcal{K}_t + q_3)(\nu_1 \mu_t + \nu_2)\Delta t. \tag{A.8}$$

The coefficients of the linearized formulations of calendar and cycle aging are presented in Table A.5. ν_2 is zero because the cycle aging is zero when the battery is not being charged or discharged.

Data availability

Data will be made available on request.

References

[1] Modig N, Eriksson R, Ruokolainen P, Ødegård JN, Weizenegger S, Fechtenburg TD. Overview of Frequency Control in the Nordic Power System. Nordic Analysis Group; 2022.

[2] kraftnät S. Information on different ancillary services. 2024, https://www.svk.se/en/stakeholders-portal/electricity-market/provision-of-ancillary-services/information-on-different-ancillary-services/ [Accessed 12 June 2024].

[3] ENTSOe. Technical requirements for frequency containment reserve provision in the Nordic Synchronous Area. Tech. rep, ENTSOe; 2023.

[4] kraftnät S. Utbud på marknaderna för reserver. 2024, https://www.svk.se/aktorsportalen/bidra-med-reserver/behov-av-reserver-nu-och-i-framtiden/utbud-pa-marknaderna-for-reserver/ [Accessed 12 June 2024].

[5] Zhao T, Parisio A, Milanović JV. Distributed control of battery energy storage systems for improved frequency regulation. IEEE Trans Power Syst 2020;35(5):3729–38. http://dx.doi.org/10.1109/TPWRS.2020.2974026.

[6] Ma Q, Wei W, Wu L, Mei S. Life-aware operation of battery energy storage in frequency regulation. IEEE Trans Sustain Energy 2023;14(3):1725–36. http://dx.doi.org/10.1109/TSTE.2023.3245197.

[7] Sofia Guzman EN, Arriaga M, Cañizares CA, Simpson-Porco JW, Sohm D, Bhattacharya K. Regulation signal design and fast frequency control with energy storage systems. IEEE Trans Power Syst 2022;37(1):224–36. http://dx.doi.org/10.1109/TPWRS.2021.3086075.

[8] Oshnoei A, Kheradmandi M, Muyeen SM. Robust control scheme for distributed battery energy storage systems in load frequency control. IEEE Trans Power Syst 2020;35(6):4781–91. http://dx.doi.org/10.1109/TPWRS.2020.2997950.

[9] Thingvad A, Ziras C, Le Ray G, Engelhardt J, Mosbæk RR, Marinelli M. Economic value of multi-market bidding in nordic frequency markets. In: 2022 international conference on renewable energies and smart technologies. REST, vol. 1, IEEE; 2022, p. 1–5. http://dx.doi.org/10.1109/REST54687.2022.10023471.

[10] Jacqué K, Koltermann L, Figgener J, Zurmühlen S, Sauer DU. The influence of frequency containment reserve on the cycles of a hybrid stationary large-scale storage system. J Energy Storage 2022;52:105040. http://dx.doi.org/10.1016/j.est.2022.105040.

[11] Krupp A, Beckmann R, Draheim P, Meschede E, Ferg E, Schuldt F, Agert C. Operating strategy optimization considering battery aging for a sector coupling system providing frequency containment reserve. J Energy Storage 2023;68:107787. http://dx.doi.org/10.1016/j.est.2023.107787.

[12] Koltermann L, Cortés MC, Figgener J, Zurmühlen S, Sauer DU. Power curves of megawatt-scale battery storage technologies for frequency regulation and energy trading. Appl Energy 2023;347:121428. http://dx.doi.org/10.1016/j.apenergy.2023.121428.

[13] Astero P, Evens C. Optimum operation of battery storage system in frequency containment reserves markets. IEEE Trans Smart Grid 2020;11(6):4906–15. http://dx.doi.org/10.1109/TSG.2020.2997924.

[14] Casla IM, Khodadadi A, Söder L. Optimal day ahead planning and bidding strategy of battery storage unit participating in nordic frequency markets. IEEE Access 2022;10:76870–83. http://dx.doi.org/10.1109/ACCESS.2022.3192131.

[15] Gao S, Li H, Jurasz J, Dai R. Optimal charging of electric vehicle aggregations participating in energy and ancillary service markets. IEEE J Emerg Sel Top Ind Electron 2022;3(2):270–8. http://dx.doi.org/10.1109/JESTIE.2021.3102417.

[16] Pavić I, Pandžić H, Capuder T. Electric vehicle aggregator as an automatic reserves provider under uncertain balancing energy procurement. IEEE Trans Power Syst 2023;38(1):396–410. http://dx.doi.org/10.1109/TPWRS.2022.3160195.

[17] Subroto RK, Gebbran D, Moreno AB, Dragičević T. BESS optimal sizing and scheduling for energy arbitrage and frequency containment reserve via dual-loop optimization. In: 2022 IEEE transportation electrification conference & expo. ITEC, IEEE; 2022, p. 941–6. http://dx.doi.org/10.1109/ITEC53557.2022.9813993.

[18] Mohamed A, Rigo-Mariani R, Debusschere V, Pin L. Stacked revenues for energy storage participating in energy and reserve markets with an optimal frequency regulation modeling. Appl Energy 2023;350:121721. http://dx.doi.org/10.1016/j.apenergy.2023.121721.

[19] Information on different ancillary services. 2024, URL https://www.svk.se/en/stakeholders-portal/electricity-market/provision-of-ancillary-services/information-on-different-ancillary-services/.

[20] Svenska Kraftnät. Villkor för Leverantör av FCR- Bilaga till Avtal om leverans av Balanstjänster. Svenska kraftnät; 2024, URL https://www.svk.se/siteassets/aktorsportalen/bsp-och-brp/aktuella-avtal-bsp-och-brp/aktuella-avtal-bsp/bsp-bilaga-2-villkor-fcr.pdf.

[21] Khezri R, Steen D, Wikner E, Tuan LA. Optimal V2G scheduling of an EV with calendar and cycle aging of battery: An MILP approach. IEEE Trans Transp Electr 2024. http://dx.doi.org/10.1109/TTE.2024.3384293, 1–1.

[22] Wang J, Purewal J, Liu P, Hicks-Garner J, Soukazian S, Sherman E, Sorenson A, Vu L, Tataria H, Verbrugge MW. Degradation of lithium ion batteries employing graphite negatives and nickel–cobalt–manganese oxide+ spinel manganese oxide positives: Part 1, aging mechanisms and life estimation. J Power Sources 2014;269:937–48. http://dx.doi.org/10.1016/j.jpowsour.2014.07.030.

[23] ENTSO-E. ENTSO-E Transparency Platform. 2024, https://transparency.entsoe.eu/ [Accessed: 07 March 2024].

[24] eSett. eSett Open data. 2024, https://opendata.esett.com/ [Accessed 07 March 2024].

[25] Fingrid. Fingrid open data. 2023, https://data.fingrid.fi/en [Accessed 07 October 2023].

[26] Calearo L, Thingvad A, Marinelli M. Modeling of battery electric vehicles for degradation studies. In: 2019 54th international universities power engineering conference. UPEC, IEEE; 2019, p. 1–6.